Discernment and Quantification of Internal and External Acid Sites on Zeolites

Qi Zhao,[†] Wen-Hua Chen,[†] Shing-Jong Huang,[†] Yu-Chih Wu,[‡] Huang-Kuei Lee,[‡] and Shang-Bin Liu*,[†]

Institute of Atomic and Molecular Sciences, Academia Sinica, P.O. Box 23-166, Taipei, Taiwan 106, R.O.C., and Institute of Materials Science and Manufacturing, Chinese Culture University, Taipei, Taiwan 111, R.O.C.

Received: October 26, 2001; In Final Form: February 10, 2002

A new methodology is reported for concurrent qualitative and quantitative characterization of internal and external acid sites in zeolitic catalysts. H−ZSM-5 zeolites with varied Si/Al ratios have been examined by solid-state ^{31}P MAS NMR using different adsorbed probe molecules, namely trimethylphosphine oxides (TMPO) and tributylphosphine oxide (TBPO), in conjunction with elemental analysis. Up to seven distinct ^{31}P resonance peaks at 86, 75, 67, 63, 53, 43, and 30 ppm were identified from the ^{31}P NMR spectra of adsorbed TMPO. The resonance peak at 30 ppm has never been observed previously and may be ascribed to mobile TMPO. The peak at 43 ppm is assigned to physisorbed TMPO. The rest of the peaks result from $TMPOH^+$ complexes at Brønsted sites with peaks at higher chemical shifts reflecting acid sites of higher strengths. ^{31}P NMR experiments, performed with TMPO and TBPO adsorbed on a mesoporous MCM-41 sample, respectively, provide further correlation of the internal and external acid sites. It is concluded that the peaks at 75 and 53 ppm arise exclusively from the internal Brønsted sites, whereas the peaks at 86, 67, and 63 ppm are associated with both internal and external acid sites. While the concentration and distribution of internal sites were found to increase with acid strengths, changing the Si/Al ratio of HZSM-5 has nearly no effect on the strength of the external acid sites.

1. Introduction

Acidity plays a key role in the catalytic performance, namely activity and selectivity, of solid acid catalysts during hydrocarbon transformation reactions.[1−3] For substrates that are smaller than the pore aperture of the catalyst, primary reactions normally have the shape-selective advantage and are catalyzed by acid sites located predominantly within the intracrystalline pores/channels of the catalysts (typical crystalline size ca. 0.1−10 μm).[2−5] Nonetheless, active sites present on the extracrystalline surface of the catalysts may provoke secondary, nonselective isomerization reactions during alkylation, disproportionation, or isomerization of, e.g., alkylbenzene, and hence are responsible for the diminution of the overall shape selectivity.[6−10] The external acid sites may also be the exclusive active centers in the reaction especially when the catalytic system is limited by reactant selectivity.[11] Thus, qualitative as well as quantitative characterization of both the internal and external acid sites are essential in understanding the detailed reaction mechanism and related selectivity features of the catalysts. However, while the characterization of the *overall* acidity of zeolites have been widely reported, there have been few reports that have discerned the internal vs external acidity, in terms of their type, strength, and concentration of the zeolite catalysts.[12−14]

Conventional methods for characterizing the acidity of solid acid catalysts normally invoke the direct observation of the acidic hydroxyl OH groups either by using IR[15−18] or ^{1}H MAS NMR[19,20] spectroscopy or through the adsorption of basic probe molecules followed by analytical or spectroscopic methods, such as titration,[21] calorimetry,[14,22−24] thermal desorption,[14,24−27] and IR or NMR spectroscopy.[10,16−18,23,26−35] Probe molecules containing elements having unpaired electrons (N, O, P etc.), e.g., ammonia, pyridine, methylamine or trimethylphosphine (TMP), are commonly used. In general, these analytical techniques are useful for quantitative determination (acid amount and strength) of the *overall* acidity. However, they cannot distinguish the types of acid sites due to accessibility and/or diffusion problems present in the catalyst.[15,36] On the other hand, conventional spectroscopic techniques are usually limited by sample preparation procedures involved and are thus more suitable for qualitative characterization, namely the discernment of Brønsted and Lewis acid sites.

A novel solid-state ^{31}P NMR technique developed recently, however, reveals the propensity in simultaneous determination of the types and strengths of acid sites in zeolites and related catalysts using trialkylphosphine[29−31] or trialkylphosphine oxide[32,33] as probes. The advantages of using these phosphorus molecules over other NMR probes, such as pyridine or methylamine, are a higher sensitivity and a wider chemical shift range (>300 ppm) possessed by the ^{31}P nucleus compared to ^{13}C or ^{15}N.[28] For example, Lunsford and co-workers[30] showed that adsorbed trimethylphosphine (TMP) molecules react with Brønsted acid sites in zeolite HY to form protonated $TMPH^+$ ionic pair complexes, as illustrated in Figure 1a, to give a ^{31}P resonance peak with a chemical shift in the range from −2 to −5 ppm, whereas the resonance responsible for TMP's interaction with Lewis acid sites is located at a higher field, typically within the range from ca. −30 to −60 ppm.

Certain drawbacks exist while using TMP as the probe molecule. First, the narrow ^{31}P chemical shift range (ca. 3 ppm) of the $TMPH^+$ complexes makes it difficult to embody various Brønsted acid sites. Second, the flammable and air-sensitive

* Corresponding author. Tel: +886-2-23668230. Fax: +886-2-23620200. E-mail: sbliu@sinica.edu.tw.
[†] Academia Sinica.
[‡] Chinese Culture University.

10.1021/jp015574k CCC: $22.00
Published on Web 03/22/2002

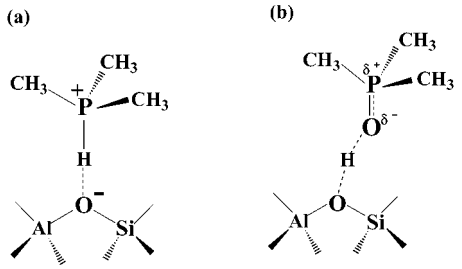

Figure 1. Schematic diagrams for the formations of (a) ion pair $TMPH^+$ complex and (b) hydrogen-bonded $TMPOH^+$ complex on the Brønsted acid sites of solid acid catalysts.

nature of TMP in bulk demands diligent and cumbersome sample preparation procedures.[29−31] In these contexts, trialkylphosphine oxides, such as trimethylphosphine oxide (TMPO)[32,33] or tributylphosphine oxide (TBPO),[10] are more preferable as probes. The sizes of TMP and of TMPO (kinetic diameter ca. 0.55 nm) are smaller than the typical pore aperture of 10-membered ring zeolites (ca. 0.60 nm) This enables them to diffuse into the intracrystalline channels/pores of the zeolites, rendering concurrent detection of both the internal and external acid sites. In comparison, the size of TBPO (ca. 0.82 nm)[37] is too large to penetrate into the channels and hence can merely detect acid sites located on the external surface of the zeolite crystallites. More importantly, in contrast to TMP, the phosphine oxide molecules, which possess partially negative-charged oxygen atoms,[38] tend to interact with the bridging hydroxyl groups (which act as proton donors) in zeolitic adsorbents to form O- -H chemical bonds, as illustrated schematically in Figure 1b for TMPO. Consequently, the density of the electron cloud surrounding the ^{31}P nucleus neighboring the oxygen atom on the phosphine oxides decreases with increasing acid strength of the Brønsted acid sites, which in turn causes the ^{31}P resonance to shift downfield.[32,33]

In this paper, we demonstrate that concurrent qualitative and quantitative characterization of internal and external acid sites on acid catalysts can be made by means of solid-state ^{31}P MAS NMR of various phosphorus probes in conjunction with ICP elemental analysis. Detailed features of the acid sites, namely their nature, location, concentration, and strength in the HZSM-5 zeolites with varied framework Al contents were determined. Complementary studies by ^{27}Al MAS NMR spectroscopy and NH_3-TPD measurements were also made.

2. Experimental Section

2.1. Materials. Powdered, binderless HZSM-5 zeolites with varied Si/Al ratios of 15, 26, and 75 were obtained from Strem Chemical Inc. The structures and framework compositions of the samples were confirmed by powder X-ray diffraction (XRD) and ^{29}Si MAS NMR. The average particle size and BET surface area of the samples were ca. 0.2−3.0 μm and 400 m^2/g, respectively, as specified by the supplier. Additional proof of internal and external acid sites was made using samples whose surface properties were modified by the silica chemical vapor deposition (Si−CVD) method. Sample silyation treatment was conducted by passing a mixture of 4 wt % TEOS in toluene through the catalyst bed at 413 K under N_2 as the carrier gas (12 mL/h) for 6 h, followed by calcination in flowing air (100 mL/min) at 823 K for 4 h. Detailed information regarding sample surface modification can be found elsewhere.[10,39] A mesoporous MCM-41 molecular sieve sample (Si/Al = 70) with particulate morphology, synthesized by the "delayed neutralization method",[40] was also used as a reference adsorbent in this study. The sample was found to possess an average pore size of 2.54 nm and a BET surface area of ca. 1,000 m^2/g, as confirmed by N_2 adsorption/desorption isotherm measurements at 77 K.

2.2. Characterization Methods. *Solid-State Multinuclear NMR.* All solid-state NMR experiments were carried out on a Bruker MSL-500P spectrometer at room temperature (298 K). ^{31}P MAS NMR spectra were acquired at the Larmor frequency of 202.46 MHz using a single-pulse sequence with a pulse width of 2 μs (ca. $\pi/5$ pulse), a recycle delay of 5 s, and a typical sample spinning frequency of 10 kHz. Typically, 700−1400 (for TMPO adsorbate) or 8000−15 000 (for TBPO) transients were accumulated to obtain a spectrum with adequate signal-to-noise (S/N) ratio. ^{31}P MAS NMR spectra with or without proton decoupling were also obtained. For the latter, the measurement was made with the $^1H \rightarrow {}^{31}P$ cross-polarization (CP) technique using a contact time of 3 ms. ^{27}Al MAS NMR spectra were obtained from hydrated HZSM-5 samples at a frequency of 130.32 MHz using a single-pulse sequence under the following conditions: sample spinning rate 5.5 kHz; pulse width 1 μs ($<\pi/6$), and recycle delay 500 ms. Aqueous 85% H_3PO_4 solution and $Al(H_2O)_6^{3+}$ were taken as external references for ^{31}P and ^{27}Al NMR chemical shifts, respectively. Prior to the adsorption of the probe molecules onto HZSM-5 (or MCM-41), the samples were dehydrated under vacuum ($<10^{-5}$ Torr; 1 Torr = 133.32 Pa) at 723 K (or 623 K) for at least 24 h. Subsequent adsorption of phosphorus probe molecules were carried out at room temperature. In the case of TMP adsorption, the adsorbate was introduced to the dehydrated HZSM-5 sample via thermal decomposition of trimethylphosphine silver iodide complex (Acros) at 473 K. The amount of TMP loading on the sample was derived from the observed pressure drop. For the adsorption of phosphine oxides, a known amount of TMPO (100%, Alfa) or TBPO (98%, Acros) dissolved in anhydrous CH_2Cl_2 was added (by a gastight syringe) into a vessel containing a dehydrated sample in a N_2 glovebox. To ensure uniform adsorption of probe molecules on the sample, the loaded sample was agitated in an ultrasonic shaker for ca. 1 h after thorough mixing, and then allowed to sit at ambient temperature for at least 12 h. Removal of the CH_2Cl_2 solvent was achieved by first extraction (under liquid N_2) and then evacuation (at 323 K). Finally, the sample vessel was placed in the N_2 glovebox where the sample was transferred into a ZrO_2 MAS rotor (4 mm o.d.) and then sealed by a gastight Kel-F cap.

ICP Elemental Analysis. Elemental analysis by ICP (Jarrell-Ash, ICAP 9000) was performed to correlate the loading of the probe molecules with the amount of acid sites on each sample. Typically, ca. 0.1 g of the adsorbate loaded sample was dissolved in 10 mL of a HF, HNO_3, and HCl mixture and then added to 60 mL of a saturated boric acid solution at room temperature. The amounts of P, Al, and Si elements were then determined using the respective commercial standards.

Ammonia-TPD. NH_3-TPD experiments were performed in a DuPont 951 TGA instrument. Typically, each sample (ca. 20 mg) was heated at a rate of 10 K/min under a N_2 gas stream (100 mL/min), calcined at 823 K for 2 h, and then cooled to 373 K while purged in NH_3 (40 mL/min). The catalyst was then exposed to NH_3 for ca. 1 h and subsequently purged with N_2 gas (100 mL/min) for ca. 0.5 h to remove the excessive NH_3. Finally, the ammonia desorption profile was recorded from 373 to 823 K at a heating rate of 10 K/min.

3. Results

3.1. ^{27}Al MAS NMR. It is well-known that the nature and concentration of Al species in aluminosilicate materials are

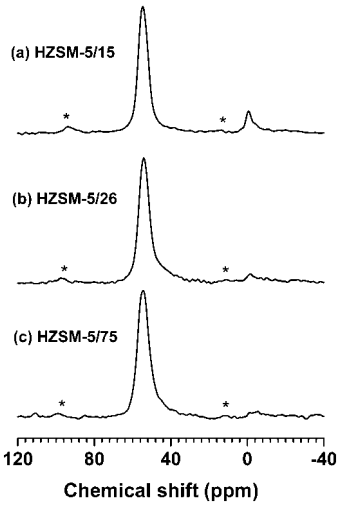

Figure 2. ^{27}Al MAS NMR spectra of HZSM-5 zeolites with Si/Al ratios of (a) 15, (b) 26, and (c) 75. The sample spinning rate is 5.5 kHz. * denotes spinning sidebands.

closely related to the acid features that are crucial for the catalytic performance of the catalysts.[2,41−43] Solid-state ^{27}Al MAS NMR is a sensitive tool commonly used for determining the coordination of Al.[44] As shown in Figure 2 for hydrated HZSM-5 zeolites with varied Si/Al ratios, the resonances at chemical shifts of 55 and 0 ppm can be assigned as due to tetrahedral (4-coordinated) framework Al and octahedral (6-coordinated) nonframework Al species, respectively. A notable decrease in the amount of extraframework Al species with decreasing Al content of zeolite was observed. Further spectral analysis indicated that more than 7% of the total Al was present in the HZSM-5/15 sample (Si/Al = 15) as extraframework Al species. In comparison, the HZSM-5/75 sample (Si/Al = 75) exhibited only a trace amount of octahedral Al species. It should be noted that, for quadrupolar nuclei of nonintegral spin such as ^{27}Al ($I = {}^5/_2$), normally only the central ($^1/_2 \leftrightarrow -{}^1/_2$) transitions are observed.[44] These transitions are independent of the first-order quadrupolar interactions. The second-order quadrupolar interaction, which is only partially averaged by the single-pulse MAS NMR experiment, may cause a broadening of the ^{27}Al resonance such that a portion of the resonance signal becomes "invisible".[45] Thus, results obtained from ^{27}Al MAS NMR studies are only capable of providing qualitative information of the presence of Al species in zeolites.

3.2. NH_3-TPD. The TPD profiles of ammonia obtained from HZSM-5 with varied Al contents are depicted in Figure 3. In general, two desorption peaks can be observed for each sample. The low-temperature peak (LT) located at ca. 473 K corresponds to NH_3 desorbing from the weaker acid sites. This peak, which is also observed for nonacidic silicalite, can be ascribed mostly due to physisorbed NH_3. The high-temperature peak (HT) at ca. 673 K corresponds to NH_3 chemisorbed at the acid sites. The area of the HT peak reflects the concentration of the acid sites, while the temperature at which the HT peak maximum occurs (T_m) reflects the *overall* acid strength of the sample.[15] It is found that the amount of acid sites decreases with a decreasing Al content in the HZSM-5 zeolites. For example, the amount of acid sites for HZSM-5 samples with Si/Al ratios of 15, 26, and 75 is found to be 0.57 ± 0.02, 0.49 ± 0.02, and 0.23 ± 0.03 mmol/g sample, respectively, whereas their *overall* acid strengths seem to follow the opposite trend.

As mentioned earlier, characterization of zeolite acidity using the TPD method has its limitations. It cannot differentiate the desorption of basic probe molecules (e.g., NH_3) from the Brønsted or the Lewis acid sites, nor can it distinguish the internal from the external acid sites. The solid-state MAS NMR studies to be discussed below are aimed to resolve these problems.

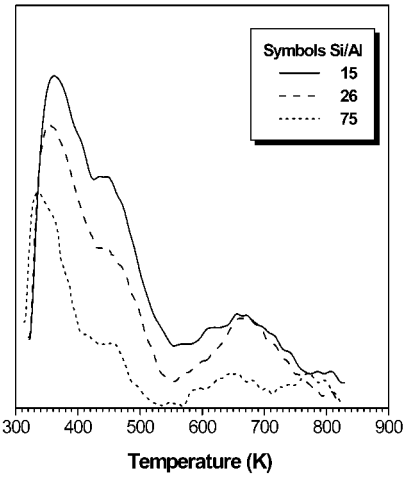

Figure 3. NH_3-TPD profiles of HZSM-5 zeolites with varied Si/Al ratios.

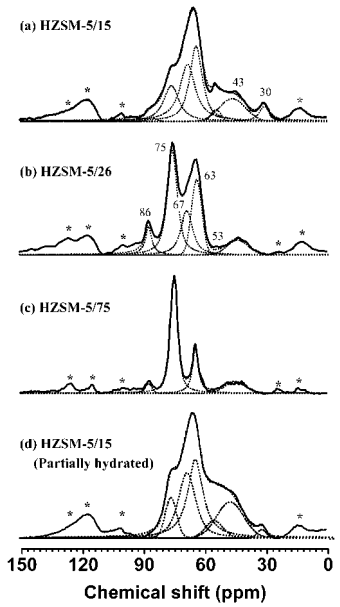

Figure 4. ^{31}P MAS NMR spectra of TMPO adsorbed on HZSM-5 zeolites with Si/Al ratios of (a) 15, (b) 26, and (c) 75. The lower spectrum in (d) was obtained from the HZSM-5/15 sample exposed to humidity for 1.5 h. The dashed curves indicate results of spectral analyses by Gaussian deconvolution. The sample spinning rate is 10 kHz. * denotes spinning sidebands.

3.3. ^{31}P MAS NMR of TMPO Adsorbed on HZSM-5 Zeolites. Parts a−c of Figure 4 display the ^{31}P MAS NMR spectra of TMPO adsorbed on various HZSM-5 zeolites with different Al contents. The results obtained from spectral analysis using the Gaussian deconvolution method (Bruker WINFIT software) are also depicted. A total of seven resonance peaks at chemical shifts of 86, 75, 67, 63, 53, 43, and 30 ppm can be identified for the HZSM-5/15 sample. Upon increasing the sample Si/Al ratio, the intensity of the peaks at the higher chemical shifts (i.e., in the downfield direction) increases and some of the characteristic peaks at high field vanish. For example, for HZSM-5/26, the resonance peaks at 53 and 30 ppm disappeared. An additional peak at 67 ppm disappeared for HZSM-5/75 (Table 1).

TABLE 1: ^{31}P NMR Chemical Shift Assignments and Distribution of Brønsted Acid Sites of HZSM-5 Zeolites Loaded with TMPO and TBPO Probe Molecules

TMPO							
chemical shift ($\Delta\delta$)[a]	**86**(*47*)	**75**(*36*)	**67**(*28*)	**63**(*24*)	**53**(*14*)	**43**(*4*)[b]	**30**[b]
sample/(Si/Al)[c]							
HZSM-5/15[d]	0.5	22.4	37.5	36.6	3.0	v	v
	(- -, 0.005)	(0.165, - -)	(0.258, 0.017)	(0.242, 0.027)	(0.021, - -)		
HZSM-5/26[d]	6.9	45.4	22.7	25.0		v	
	(0.014, 0.010)	(0.159, - -)	(0.067, 0.012)	(0.063, 0.025)			
HZSM-5/75[d]	3.5	69.8		26.7		v	
	(0.003, 0.002)	(0.108, - -)	(- -, 0.002)	(0.032, 0.009)			
TBPO							
chemical shift ($\Delta\delta$)[a]	**92**(*45*)		**75**(*28*)	**71**(*24*)		**54**(*7*)[b]	**47**[b]
sample/(Si/Al)[c]							
HZSM-5/15[e]	10.5		35.0	54.5			
HZSM-5/26[e]	22.3		25.2	52.5			
HZSM-5/75[e]	15.4		17.6	67.0		v	v

[a] Data in bold denote chemical shifts of characteristic peaks (±1 ppm); the italic numbers in parentheses ($\Delta\delta$) refer to the corresponding chemical shift differences with respect to crystalline TMPO (39 ppm) or TBPO (47 ppm). [b] The sign v indicates the appearance of characteristic peak. [c] Value under slash at the end of notation represents sample Si/Al ratio. [d] Values on top represent relative concentration of acid sites (%); data in parentheses (int, ext) give the amounts of internal and external acid sites (±0.001 mmol/g cat.), respectively. [e] Values specifically represent relative concentration of external acid sites (%).

The ^{31}P resonances at 86, 75, 67, 63, and 53 ppm can be assigned a priori to TMPO adsorbed on Brønsted acid sites of HZSM-5 zeolites.[32,33] This assignment is supported by the results obtained from the same series of samples using TMP adsorbates (see below). To verify the origin of the resonances, additional experiments were performed. This is done by exposing the TMPO loaded samples to humidity, as illustrated for HZSM-5/15 in Figure 4d. Upon introducing H_2O to the sample, the intensity of the peak at 43 ppm is increased while there is a slight decrease in the intensity of the peaks at 86, 75, 67, and 63 ppm. It is known that Lewis acid sites (tricoordinated Al species in zeolites), which weakly interacted with TMPO, may easily react with H_2O to form weak Brønsted acid sites. However, the strong hydrogen bonding between TMPO and the Brønsted acid sites is unlikely to be dissociated when in the presence of H_2O. Consequently, only those ^{31}P resonances associated with Lewis acid sites will be diminished upon further hydration of the sample. The justification and assignment of the peak at 30 ppm will be discussed later.

3.4. ^{31}P MAS NMR of TMP Adsorbed on H−ZSM-5 Zeolites. The room temperature ^{31}P MAS NMR spectra of the TMP loaded samples obtained with and without proton decoupling and under ^{1}H→^{31}P CP conditions are depicted in Figure 5, illustrated for H−ZSM-5/26 and H−ZSM-5/75 samples, which reveal similar results. The spectra obtained in the absence of proton decoupling typically reveal five characteristic peaks at −3.2, −5.5, −50.4, −59.3, and −62.2 ppm. The peaks at −3.2 and −5.5 ppm collapsed to a single peak at −4.5 ppm when proton-decoupling was applied. Together with the observation of *J*-coupling between the ^{31}P and ^{1}H nuclei (ca. 550 Hz),[46] this is indicative that the P atoms on the TMP are coupled to the proton of the bridging silanol OH groups (Brønsted acid sites) in the zeolite samples. Accordingly, when the experiment was carried out under CP conditions, the intensity of the singlet at −4.5 ppm is increased.

3.5. ^{31}P MAS NMR of TBPO Adsorbed on HZSM-5 Zeolites. Unlike ^{31}P MAS NMR studies invoking TMP or TMPO probes, which are capable of characterizing internal and external acid sites, the adoption of TBPO as a probe can only detect acid sites located on the extracrystalline surfaces of the HZSM-5 samples. This is, of course, due to the large molecular size of the TBPO, which makes it too big to enter the channels of the HZSM-5 zeolites. The ^{31}P MAS NMR of TBPO adsorbed on various HZSM-5 samples with different Al contents are displayed in Figure 6a−c. Up to five characteristic peaks located at 92, 75, 71, 54, and 47 ppm were observed for the HZSM-5/75 sample (Table 1). For the samples HZSM-5/15 and HZSM-5/26, the resonances at 54 and 47 ppm were either invisible or negligibly small. ^{31}P MAS NMR of bulk TBPO crystalline samples revealed only a single peak at 47 ppm (not shown). Hence, the resonance with the lowest chemical shift at 47 ppm in Figure 6c can be assigned unambiguously as due to crystalline TBPO. Upon further exposing the adsorbate-loaded sample to humidity, as illustrated by the sample HZSM-5/26 in Figure 6d, the ^{31}P spectra remain practically unchanged. Such observations provide additional support to the assignment of the resonance peaks to be discussed later. Finally, the observed chemical shift and the intensity of the peaks resulting from the external acid sites remain practically unchanged upon increasing the Si/Al ratio of the samples.

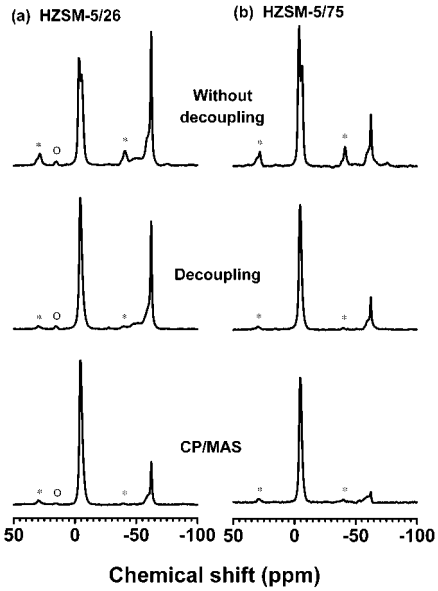

Figure 5. ^{31}P MAS NMR spectra of TMP adsorbed on (a) HZSM-5/26 (loading 0.64 mmol/g sample) and (b) HZSM-5/75 (loading 0.23 mmol/g sample) obtained with different experimental methods: (top) without proton decoupling; (center) with proton decoupling; (bottom) with ^{1}H → ^{31}P cross polarization. The sample spinning rate is 7 kHz. * and ○ denotes spinning sidebands and trace impurities, respectively.

3.6. ^{31}P MAS NMR of TMPO Adsorbed on Silylated HZSM-5 Zeolites. The effect of sample surface modification

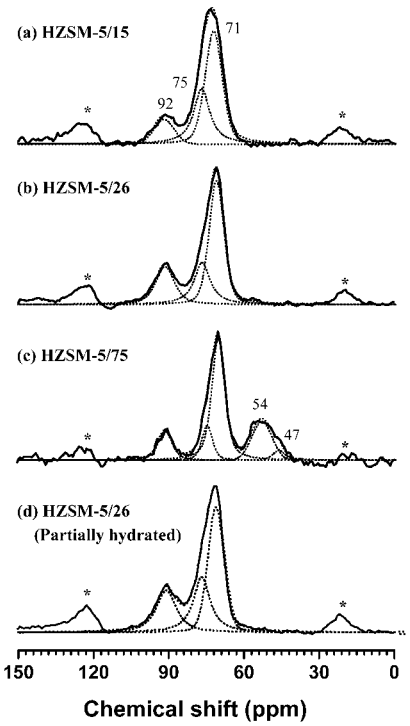

Figure 6. Similar to Figure 4, but obtained with TBPO adsorbed on HZSM-5 zeolites.

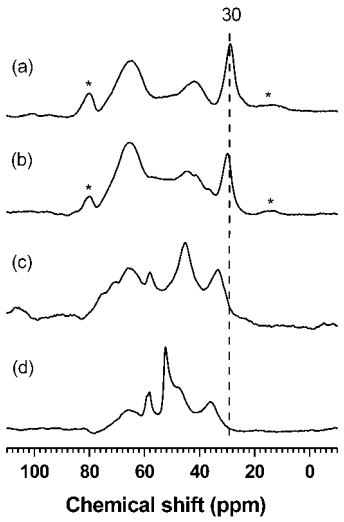

Figure 7. Variations of ^{31}P MAS NMR spectra for TMPO adsorbed on silylated HZSM-5/15 sample (prepared by Si−CVD method) (a) before and (b)−(d) after partial hydration treatment done by exposing the adsorbate loaded sample to humidity for (b) 1.5 h, (c) 4.5 h, and (d) 30 h. * denotes spinning sidebands.

on the distribution of acid sites was investigated. This was achieved by surface silylation treatment of the sample by Si−CVD using TEOS as the agent. It has been shown that Si−CVD silylation treatment is effective in deactivating the external acid sites while keeping the internal acid sites intact.[8,10,39] However, this effect cannot readily be confirmed on the basis of the observed ^{31}P MAS NMR results alone. Indeed, similar spectra were obtained from TMPO adsorbed on the parent (Figure 4a) and the silylated (Figure 7a) HZSM-5/15 samples. This can be a priori ascribed as mainly due to the fact that the external acid site accounts for less than ca. 7% of the total acidity (see below) in the HZSM-5 samples used in this study.

Upon progressive exposure of the silylated sample loaded with TMPO to humidity, the chemical shift of the intense sharp peak originally at 30 ppm moved toward downfield. This is exemplified by the surface-modified H−ZSM-5/15 sample, which was subjected to Si-CVD treatment for 6 h in Figure 7. When a nearly saturated amount of water was coadsorbed, as illustrated by the ^{31}P NMR spectrum in Figure 7d for the sample subjected to a prolonged (30 h) humidity exposure, the resonance at 30 ppm in Figure 7a (for dehydrated sample) shifted to a lower field. In the meantime, line narrowing of the other peaks occurred and appeared to move toward the high-field direction.

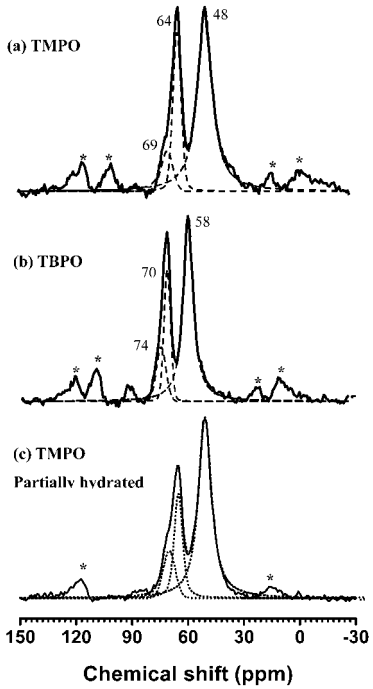

Figure 8. ^{31}P MAS NMR spectra of (a) TMPO and (b) TBPO adsorbed on a mesoporous AlMCM-41 sample (Si/Al = 70, averaged pore size 2.54 nm). The lower spectrum in (c) was obtained from the TMPO/MCM-41 sample exposed to humidity for 1.5 h. The dashed curves indicate results of spectral analyses by Gaussian deconvolution. The sample spinning rate is 10 kHz. * denotes spinning sidebands.

3.7. ^{31}P MAS NMR of TMPO and TBPO Adsorbed on AlMCM-41. Parts a and b of Figure 8 display the ^{31}P MAS NMR spectra of TMPO and TBPO adsorbed on a mesoporous AlMCM-41 molecular sieve sample. The spectrum of the TMPO/MCM-41 system revealed three characteristic resonance peaks at 69, 64, and 48 ppm. Similarly, three peaks were observed for the TBPO/MCM-41 system but with different chemical shifts at 74, 70, and 58 ppm. The variation in ^{31}P NMR chemical shifts observed for the two systems reflect the different local environments experienced by the two adsorbed phosphine oxide homologues. The peaks at 48 and 58 ppm can be unambiguously attributed to physisorbed TMPO[32] and TBPO,[10] respectively, whereas the two peaks observed (for both systems) at lower field are ascribed as due to interaction of the phosphine oxides probe molecules with Brønsted acid sites located at two different environments. This argument is supported by the ^{31}P NMR results of partially hydrated adsorbate-loaded samples in which only a marginal decrease in the corresponding peak intensities was observed.

4. Discussion

4.1. Qualitative Interpretation of ^{31}P NMR Chemical Shifts and Acid Sites for HZSM-5 Zeolites. *Assignment of ^{31}P NMR Chemical Shifts.* Most solid-state ^{31}P NMR studies in the existing literature concerning acidity characterization of

zeolites and related catalysts were made using the adsorption of the TMP probe molecule.[29,30] As shown in Figure 5, ^{31}P NMR spectra obtained from TMP/HZSM-5 systems typically reveal up to five characteristic peaks at −3.2, −5.5, −50.4, −59.3, and −62.2 ppm. Complementary experiments, either proton decoupling or $^{1}H \rightarrow {}^{31}P$ cross-polarization, during NMR acquisition reveal that the doublet at −3.2 and −5.5 ppm collapses to form a single peak (at −4.5 ppm) and provide direct evidence that the TMP probe molecules are coupled to the Brønsted acid sites. Since only resonances corresponding to immobile species can be enhanced by CP/MAS in the NMR time scale,[44] the other peaks whose intensities are diminished during the experiment are likely due to mobile or weakly adsorbed TMP. By comparing with neat TMP, which reveals a single resonance at −63 ppm,[30] the peaks at −59.4 and −62.2 ppm observed for the TMP/HZSM-5 system can be attributed to physisorbed and liquidlike TMP, respectively.

The assignment of the weak peak at −50.4 ppm, however, demands further justification. Lunsford and co-workers attributed[30] the resonances in the range of −32 to −58 ppm observed in the zeolites HY to TMP associated with tricoordinated Al^{3+} Lewis acid sites. However, on the basis of our results obtained from the partially hydrated samples, the presence of Lewis acidity cannot be justified. In view of the large basicity possessed by the TMP ($pK_b = 5.35$)[30] as compared to TMPO ($pK_b = 14.5$),[47] the TMP probe molecule should be more preferable to form Lewis complexes with Al^{3+}. However, a rapid exchange between the adsorbed TMP and liquidlike TMP may exist, making it difficult to quantify the TMP that are weakly adsorbed on Lewis acid sites. That the peak intensity at −50.4 ppm is relatively weak in the ^{31}P NMR spectra of the TMP/HZSM-5 systems (Figure 5) and that all characteristic peaks remain intact upon partial hydration of the TMPO/HZSM-5 samples (see Figure 4) indicate that the concentration of Lewis acid sites in the HZSM-5 sample will be negligibly small compared to Brønsted acid sites.

For the TMPO/HZSM-5 systems, up to seven characteristic peaks at 86, 75, 67, 63, 53, 43, and 30 ppm were identified from the observed ^{31}P MAS NMR spectra (Figure 4). The resonances at 86, 75, 67, 63, and 53 ppm have been assigned as due to TMPO adsorbed on the Brønsted acid sites of the HZSM-5 zeolites.[32,33] Among these, the assignment of the peak at 53 ppm is somewhat more controversial. Maciel and co-workers,[29] who also observed the resonance at 53 ppm for TMPO/silica−alumina system, assigned the peak to TMPO associated with Lewis acidity. However, this resonance was not observed by Rakiewicz et al.[32] in a similar system that contained 13% Al in a silica−alumina catalyst. Nevertheless, the latter authors observed a similar peak at 53 ppm for TMPO adsorbed on γ-alumina and at 55 ppm for HY (Si/Al = 2.8) and USY (Si/Al = 2.9, 8.3) catalysts even when the systems were partially hydrated. Unlike the formation of a $TMPOH^+$ complex in the case of TMPO adsorption, which invokes the formation of O- - H chemical bonds, the $TMPH^+$ complex is formed by directly bonding the phosphorus atom in TMP to the proton of a Brønsted acid site (Figure 1). Thus, the corresponding change in the electronic environment at the ^{31}P nucleus of $TMPH^+$ should be larger when compared to $TMPOH^+$. As a result, a greater difference in chemical shift ($\Delta\delta$) for $TMPH^+$ vs neat TMP should be observed as compared to that of $TMPOH^+$ vs crystalline TMPO. For example, for the TMP/HZSM-5 system, a typical value of $\Delta\delta \sim 57-60$ ppm was observed for TMP associated with the Brønsted acid sites, whereas in the case of adsorbed TMPO, the $\Delta\delta$ values vary from 14 to 47 ppm (Table 1). By the same token, the $\Delta\delta$ value for TMPO adsorbed on Lewis acid sites should be smaller than the value obtained when using TMP as a probe, which is observed to be 12.6 ppm for TMP/HZSM-5 in this study. Therefore, following the conclusion made by Rakiewicz et al.[32] for TMPO adsorbed on HY and USY, we assign the 53 ppm peak observed in the TMPO/HZSM-5 systems to TMPO associated with the Brønsted acid sites. Since resonances occurring at higher chemical shifts reflect acid sites having higher acid strengths, the multiple resonance peaks by TMPO above 53 ppm observed in the present study thus indicate the existence of a stronger Brønsted acidity for zeolite HZSM-5 than USY (or HY) where only two ^{31}P NMR resonances, at 55 and 65 ppm, were observed.

Now, let us discuss the ^{31}P resonance peaks at 43 and 30 ppm observed in the TMPO/HZSM-5 system (Figures 4 and 7). First, the absence of signal at 39 ppm in the spectra for various HZSM-5 (and MCM-41) samples indicates that none of the excess TMPO adsorbed in the samples exists as crystalline bulks. Second, that the peak at 43 ppm remains visible upon partial hydration of the TMPO/HZSM-5 system (Figure 4d) favors its assignment to physisorbed TMPO. A similar observation was also found for the TMPO/USY system by Rakiewicz et al.[32] Using a more sophisticated $^{1}H/^{31}P/^{27}Al$ triple-resonance TRAPDOR[48] NMR technique, the authors showed that the resonance at 43 ppm is not associated with Al species in the zeolite.

The relatively sharp resonance peak at 30 ppm is observed for the first time and is visible only in the system of TMPO on HZSM-5/15 (Figures 4 and 7). Although Haw et al.[49] observed a peak at 27 ppm while investigating TMP adsorbed on sulfated zirconia catalysts using the same technique and ascribed the peak to the formation of $P(CH_3)_4^+$ species, such species are unlikely to exist in the TMPO/HZSM-5 system. The fact that this resonance remained practically unchanged before (Figure 4a) and after (Figure 7a) sample surface modification by Si−CVD seems to exclude the possibility that it is due to TMPO adsorbed on the external acid sites. Moreover, partial hydration of the samples (see Figure 4d and Figure 7) resulted in a downfield shift of the ^{31}P resonance, reflecting a close association of TMPO with water in the system. Thus, the peak at 30 ppm, which has a lower chemical shift compared to both physisorbed (43 ppm) and crystalline (39 ppm) TMPO, is likely due to "mobile" TMPO that either is attached in the intercrystalline voids or is weakly adsorbed near the opening of the channel pores of the zeolites.

Unlike TMPO (or TMP) in which the features of the internal and external acid sites can be obtained by ^{31}P NMR, acid sites located in the intracrystalline channels of the HZSM-5 zeolites are inaccessible to the TBPO molecules. TBPO can only interact with acid sites on the external surfaces. The ^{31}P NMR spectra obtained from the TBPO/HZSM-5 systems (Figure 6) revealed that up to five characteristic peaks located at 92, 75, 71, 54, and 47 ppm were present. We note that ^{31}P NMR peak assignments for TBPO adsorbed on solid acid catalysts are not available except in our recent paper on the effects of surface modification on product selectivity of HZSM-5 zeolites during alkylbenzene disproportionation.[10] Here, the resonance at 47 ppm can be assigned to crystalline TBPO, as evidenced by additional ^{31}P MAS NMR of bulk TBPO crystalline samples. By analogy of the peak assignments for its TMPO homologue discussed above, we ascribe the resonance peaks located at 92, 75, and 71 ppm to TBPO adsorbed on Brønsted acid sites, and the peak at 54 ppm to physisorbed TBPO. These assignments are supported by the results obtained from the systems of TBPO adsorbed on HZSM-5/26 (Figures 6b,d), which show that the spectrum remains practically unchanged upon partial hydration of the system.

TABLE 2: Assignments of ^{31}P NMR Chemical Shifts for TMPO and TBPO Adsorbed on Mesoporous MCM-41 Molecular Sieve

	δ_c	δ_1 ($\delta_1 - \delta_c$)	δ_2 ($\delta_2 - \delta_c$)
probe molecule			
TMPO	**39**	**69**(*30*)	**64**(*25*)
TBPO	**47**	**74**(*27*)	**70**(*23*)

[a] Data in bold denote chemical shifts of characteristic peaks (±1 ppm); the italicized numbers in parentheses ($\Delta\delta = \delta_1 - \delta_c$ or $\delta_2 - \delta_c$) refer to the chemical shift differences with respect to characteristic peak (δ_c) for crystalline TMPO or TBPO.

Effect of Sample Al Content. For the TMPO/HZSM-5 system, spectra shown in Figures 4a−c clearly indicate that, upon increasing the sample Si/Al ratio, the intensity of the peaks responsible for Brønsted acid sites at lower fields (86 and 75 ppm) increased accordingly while the peaks at higher fields either diminished or vanished. This provides support to the general notion that lowering of the Al content in zeolites results in an overall decrease of acid concentration and in an increase of the overall acid strengths.[2,41−43] The observation is also in accord with the NH_3-TPD results shown in Figure 3. On the other hand, the chemical shifts and peak intensities observed for TBPO/HZSM-5 systems in Figures 6a−c remain practically unchanged upon varying the Si/Al ratio of the samples, indicating that the strength and concentration of the *external* acid sites are independent of the Al content of HZSM-5 zeolites.

4.2. Discernment of Internal and External Acid Sites. As mentioned earlier, ^{31}P NMR results obtained from the TBPO/ZSM-5 systems exclusively provide information of acid sites locating on the external surfaces, whereas for the TMPO/HZSM-5 systems, features of both the internal and external acid sites can be obtained. Combining the results obtained separately from the two homologous probe molecules thus may facilitate the discernment of internal and external acidity. However, owing to the differences in the physical and chemical properties possessed by TMPO and TBPO, additional information is required before the ^{31}P chemical shifts observed from respective experiments can be correlated. This is made possible by performing experiments on a mesoporous MCM-41 sample (Si/Al = 70), which possesses a big enough pore size (2.54 nm) to accommodate both types of probe molecules.

As shown in Figure 8a, the ^{31}P NMR spectrum of TMPO/MCM-41 reveals three resonance peaks at 69, 64, and 48 ppm. Similarly, three peaks at 74, 70, and 58 ppm are observed for TBPO/MCM-41 (Figure 8b). Among these characteristic resonances, the peaks at 48 and 58 ppm can be unambiguously attributed to physisorbed TMPO and TBPO, respectively. Taking the value of the chemical shift for crystalline TMPO (39 ppm) and TBPO (47 ppm) as the reference, it is interesting to note that the corresponding difference in chemical shift, $\Delta\delta$, is nearly the same, regardless of the type of adsorbate that is present. Apparently, the change in electron density surrounding the ^{31}P nuclei in the two homologous probe molecules is rather similar at a given acid site. In other words, the $\Delta\delta$ value mainly reflects the strength of the O- -H bond between the proton of the Brønsted acid site and the oxygen atom on the adsorbed probe molecule. By comparison, the chain length of the alkyl group on the phosphine oxide has nearly no effect on $\Delta\delta$. Separate ^{1}H MAS NMR experiments on the two guest/host systems (not shown) performed recently in this laboratory have provided additional support to this argument. With regard to $\Delta\delta$, the values for the two characteristic acid peaks in the TMPO/MCM-41 system were 30 and 25 ppm, whereas for the TBPO/MCM-41 system the values of 27 and 23 ppm were observed (Table 2). By the same token, the $\Delta\delta$ values corresponding to each acid site for various H−ZSM-5 samples in the presence of different probe molecules can be deduced, as depicted in Table 1. In view of the similar $\Delta\delta$ values (and hence similar acid strength) derived, it is indicative that the peaks at 86, 67, and 63 ppm obtained from the TMPO/HZSM-5 systems correspond respectively to the peaks at 92, 75, and 71 ppm from the TBPO/HZSM-5 systems.

Consequently, since the three major ^{31}P resonances observed for the TBPO/HZSM-5 systems arise from the external acid sites, it may be concluded that the additional two peaks observed for the TMPO/HZSM-5 systems at 75 and 53 ppm should arise exclusively from the internal acid sites, whereas the peak at 86 ppm (corresponding to the 92 ppm peak in the TBPO/HZSM-5 system) is due to external acid sites. Comparing to the ^{31}P NMR resonance of TMPO dissolved in dense H_2SO_4, which shows single peak at a chemical shift of 83 ppm,[32] the acidic strength corresponding to the 86 ppm peak in the TMPO/HZSM-5 system is thus slightly stronger. This peak, which corresponds to the highest acid strength in HZSM-5 zeolites, is likely due to Brønsted acid sites located near the entrance to the pores of the HZSM-5 zeolites. At this location there are additional electrostatic interactions that may be associated with structural irregularities or defects.

4.3. Quantitative Determination of Acid Sites. The characteristics of the ^{31}P NMR resonance observed using various phosphorus probe molecules adsorbed on different samples can be quantified by correlation with the analytic results of Al, Si, and P elemental concentrations using ICP. Together with information on the relative peak areas derived by Gaussian deconvolution of the observed ^{31}P spectrum, the distribution of each acid site on various HZSM-5 samples can be estimated by taking the total peak area responsible for acid sites as 100%. The result is shown in Table 1. For example, for TMPO adsorbed on HZSM-5/15, the relative concentrations of the Brønsted acid sites corresponding to the ^{31}P NMR characteristic peaks at 86, 75, 67, 63, and 53 ppm are 0.5, 22.4, 37.5, 36.6, and 3.0%, respectively. In the case of TBPO, the relative concentrations corresponding to the three resonances at 92, 75, and 71 ppm are found to be 10.5, 35.0, and 54.5%, respectively.

Finally, by incorporating the ^{31}P NMR results obtained using appropriate probe molecules, namely, the aforediscussed TMPO and TBPO, additional valuable information on concentrations of internal *and* external acid sites can be certified. Consequently, the relative concentrations of internal vs external acid sites with identical acid strength (i.e., those having the same chemical shift; see Table 1) can further be quantified. For example, for the system of TMPO adsorbed on HZSM-5/15, the amounts of internal vs external acid sites (in mmole per gram of catalyst), denoted in Table 1 as (int, ext), for the characteristic peaks at 86, 67, and 63 ppm are determined to be (- -, 0.005), (0.258, 0.017), and (0.242, 0.027), respectively. For the ^{31}P resonances at 75 and 53 ppm, which have been ascribed exclusively as due to *internal* Brønsted acidity, the corresponding (int, ext) values are (0.165, - -) and (0.021, - -), respectively. It is noted that, for HZSM-5/15, external acid sites contribute predominantly to the ^{31}P resonance at 86 ppm, which reflects the highest acid strength in HZSM-5 zeolites. Detailed acid features for HZSM-5/26 and HZSM-5/75 samples are also depicted in Table 1.

Accordingly, the amount of total internal vs external acid sites (in mmol/g of sample) can also be calculated. We denote the respective total acidity by [int, ext] as a matter of convenience and the values [0.686, 0.049], [0.303, 0.047], and [0.143, 0.013] were derived. These values correspond to an *overall* acidity (sum of int and ext) of 0.735, 0.350, and 0.156 mmol/g of catalyst, for HZSM-5 samples with Si/Al ratios of 15, 26, and 75,

respectively. These results may be compared with the data obtained from NH_3-TPD experiments in which the corresponding *overall* amounts of acid sites for HZSM-5 samples with increasing Si/Al ratio were respectively determined as 0.57, 0.49, and 0.23 mmol/g of sample. However, it should be noted that the values so obtained represent only Brønsted acid sites detectable by the TMPO (or TBPO) probe molecules using ^{31}P NMR. Considering that each framework Al atom is charge balanced by a proton in HZSM-5 zeolites, a more detailed analysis shows that only 69, 54, and 70% of the total Brønsted acidity were detected in samples with Si/Al ratios of 15, 26, and 75, respectively. Taking this into account, it may be concluded that only 5−7% of the total acidity is contributed by acid sites located on the external surfaces of the HZSM-5 samples examined in this study.

5. Conclusions

We have demonstrated that detailed acid features of solid acid catalyst, viz. the nature, location, concentration, and strength of acid sites, may be determined by a combination of elemental analysis and ^{31}P MAS NMR of adsorbed phosphorus probe molecules. In particular, the distribution and concentration of internal vs external acidity can be differentiated by incorporating ^{31}P NMR results obtained from a suitable choice of phosphine oxide probe molecules, as illustrated in this study using TMPO and TBPO. Up to five Brønsted acid sites with varied acid strengths were identified for HZSM-5 zeolites. Two of the five were found exclusively due to internal sites and three were found to be associated with external sites. The concentrations of internal Brønsted sites having weaker acid strength were found to decrease with decreasing Al content, while those with stronger acid strengths, to increase accordingly. In contrast, for Brønsted sites located at external surfaces of HZSM-5 zeolites, their acid strengths were found to be nearly independent with the Al contents.

The methodology for discernment and quantification of internal and external acidity reported here should shed some light on the further understanding of the reaction mechanism and related selectivity features of the zeolitic catalysts during hydrocarbon transformation reactions, especially during disproportionation, alkylation or isomerization of alkylbenzenes.

Acknowledgment. We thank Drs. W. Reusch, K. T. Mueller, J. P. Osegovic, and Andy Kung for helpful discussions. This work was supported by National Science Council, R.O.C. (NSC89-2113-M-001-102).

References and Notes

(1) Venuto, P. B. *Adv. Chem. Ser.* **1971**, *102*, 260.

(2) Corma, A. *Chem. Rev.* **1995**, *95*, 559.

(3) Vaughan, D. E. W. *Properties and Applications of Zeolites*; Townsend, R. P., Ed.; Soc. Chem. Ind.: London, 1980; p 294.

(4) (a) Triantafillidis, C. S.; Evmiridis, N. P.; Nalbandian, L.; Vasalos, I. A. *Ind. Eng. Chem. Res.* **1999**, *38*, 916. (b) Triantafillidis, C. S.; Evmiridis, N. P. *Ind. Eng. Chem. Res.* **2000**, *39*, 3233.

(5) Sahoo, S. K.; Viswanadham, N.; Ray, N.; Gupta, J. K.; Singh, I. D. *Appl. Catal. A* **2001**, *205*, 1.

(6) Chen, N. Y.; Degnan, T. F.; Smith, C. M. *Molecular Transport and Reaction in Zeolites: Design and Application of Shape Selective Catalysts*; VCH Publishers: New York, 1994.

(7) Melson, S.; Schüth, F. *J. Catal.* **1997**, *170*, 46.

(8) Kunieda, T.; Kim, J. H.; Niwa, M. *J. Catal.* **1999**, *188*, 431.

(9) Tsai, T. C.; Liu, S. B.; Wang, I. *Appl. Catal. A* **1999**, *181*, 355.

(10) Chen, W. H.; Tsai, T. C.; Jong, S. J.; Zhao, Q.; Tsai, C. T.; Lee, H. K.; Wang, I.; Liu, S. B. *J. Mol. Catal. A* **2002**, *181*, 41.

(11) Haag, W. O.; Lago, R. M.; Weisz, P. B. *Faraday Discuss., Chem. Soc.* **1982**, *72*, 317.

(12) Guisnet, M. *Acc. Chem. Res.* **1990**, *23*, 392.

(13) Carniti, P.; Gervasini, A.; Auroux, A. *J. Catal.* **1994**, *150*, 274.

(14) (a) Chronister, C. W.; Drago, R. S. *J. Am. Chem. Soc.* **1993**, *115*, 793. (b) Drago, R. S.; Dias, S. C.; Torrealba, M.; de Lima, L. *J. Am. Chem. Soc.* **1997**, *119*, 4444.

(15) Van Hooff, J. H. C.; Roelofsen, J. W. *Stud. Surf. Sci. Catal.* **1991**, *58*, 241.

(16) Ward, J. W. In *Zeolite Chemistry and Catalysis*; Rabo, J. A., Ed.; ACS Monograph 171; American Chemical Society: Washington, DC, 1976; pp 118−284.

(17) Lercher, J. A.; Gründling, C.; Eder-Mirth, G. *Catal. Today* **1996**, *27*, 353.

(18) Kustov, L. M. *Top. Catal.* **1997**, *4*, 131.

(19) Pfeifer, H.; Freude, D.; Hunger, M. *Zeolites* **1985**, *5*, 274.

(20) Hunger, M. *Catal. Rev.-Sci. Eng.* **1997**, *39*, 345.

(21) Moscou, L.; Moné, R. *J. Catal.* **1973**, *30*, 417.

(22) Auroux, A.; Védrine, J. C. *Stud. Surf. Sci. Catal.* **1985**, *20*, 311.

(23) Védrine, J. C.; Auroux, A.; Bolis, V.; Dejaifve, P.; Naccache, C.; Wierzchowski, P.; Derouane, E. G.; Nagy, J. B.; Gilson, J. P.; van Hooff, J. H. C.; van den Berg, J. P.; Wolthuizen, J. *J. Catal.* **1979**, *59*, 248.

(24) Kapustin, G. I.; Brueva, T. R.; Klyachko, A. L.; Beran, S.; Wichterlová, B. *Appl. Catal.* **1988**, *42*, 239.

(25) (a) Narayanan, S.; Deshpande, K. *Appl. Catal. A* **1996**, *135*, 125. (b) Narayanan, S.; Sultana, A.; Thinh Le, Q.; Auroux, A. *Appl. Catal. A* **1998**, *168*, 373.

(26) Topsøe, N. Y.; Pedersen, K.; Derouane, E. G. *J. Catal.* **1981**, *70*, 41.

(27) Jacobs, P. A.; Martens, J. A.; Weitkamp, J.; Beyer, H. K. *Faraday Discuss. Chem. Soc.* **1981**, *72*, 353.

(28) Maciel, G. E.; Ellis, P. D. In *NMR Techniques in Catalysis*; Bell, A. T., Pines, A., Eds.; Marcel Dekker: New York, 1994; pp 231−309.

(29) (a) Baltusis, L.; Frye, J. S.; Maciel, G. E. *J. Am. Chem. Soc.* **1986**, *108*, 7119. (b) Baltusis, L.; Frye, J. S.; Maciel, G. E. *J. Am. Chem. Soc.* **1987**, *109*, 40.

(30) (a) Lunsford, J. H.; Rothwell, W. P.; Shen, W. *J. Am. Chem. Soc.* **1985**, *107*, 1540. (b) Lunsford, J. H. *Top. Catal.* **1997**, *4*, 91. (c) Zhao, B.; Pan, H.; Lunsford, J. H. *Langmuir* **1999**, *15*, 2761.

(31) Hu, B.; Gay, I. D. *Langmuir* **1999**, *15*, 477.

(32) Rakiewicz, E. F.; Peters, A. W.; Wormsbecher, R. F.; Sutovich, K. J.; Mueller, K. T. *J. Phys. Chem. B* **1998**, *102*, 2890.

(33) Osegovic, J. P.; Drago, R. S. *J. Phys. Chem. B* **2000**, *104*, 147.

(34) Biaglow, A. I.; Šepa, J.; Gorte, R. J.; White, D. *J. Catal.* **1995**, *151*, 373.

(35) Fărcaşiu, D.; Ghenciu, A. *Prog. Nucl. Magn. Reson. Spectrosc.* **1996**, *29*, 129.

(36) Gruver, V.; Panov, A.; Fripiat, J. J. *Langmuir* **1996**, *12*, 2505.

(37) Webster, C. E.; Drago, R. S.; Zerner, M. C. *J. Am. Chem. Soc.* **1998**, *120*, 5509.

(38) Engelhardt, L. M.; Raston, C. L.; Whitaker, C. R.; White, A. H. *Aust. J. Chem.* **1986**, *39*, 2151.

(39) Wang, I.; Ay, C. L.; Lee, B. J.; Chen, M. H. *Proc. 9th Int. Congr. Catal.* **1988**, 324.

(40) (a) Lin, H. P.; Cheng, S.; Mou, C. Y. *Microporous Mater.* **1996**, *10*, 111. (b) Mou, C. Y.; Lin, H. P. *Pure Appl. Chem.* **2000**, *72*, 137.

(41) Van Santen, R. A.; Kramer, G. J. *Chem. Rev.* **1995**, *95*, 637.

(42) Derouane, E. G.; Fripiat, J. G. *Zeolites* **1985**, *5*, 165.

(43) Olson, D. H.; Kokotallo, G. T.; Lawton, S. L.; Molor, W. M. *J. Am. Chem. Soc.* **1981**, *85*, 2238.

(44) Engelhardt, G.; Michel, D. *High-Resolution Solid-State NMR of Silicates and Zeolites*; Wiley: New York, 1987.

(45) Freude, D.; Haase, J. *Nucl. Magn, Reson. Basic Principles Prog.* **1993**, *29*, 1.

(46) Schoonheyde, R. A.; Van Wouwe, D.; Leerman, H. *Zeolites* **1982**, *2*, 109.

(47) (a) Hadži, D.; Klofutar, C.; Oblak, S. *J. Chem. Soc. A* **1968**, 905. (b) Arnett, E. M.; Mitchell, E. J.; Murty, T. S. S. R. *J. Am. Chem. Soc.* **1974**, *96*, 3875.

(48) (a) Van Eck, E. R. H.; Janssen, R.; Maas, W. E. J. R.; Veeman, W. S. *Chem. Phys. Lett.* **1990**, *174*, 428. (b) Grey, C. P.; Veeman, W. S.; Vega, A. J. *J. Chem. Phys.* **1993**, *98*, 7711. (c) Grey, C. P.; Vega, A. J. *J. Am. Chem. Soc.* **1995**, *117*, 8232.

(49) Haw, J. F.; Zhang, J. H.; Shimizu, K.; Venkatraman, T. N.; Luigi, D. P.; Song, W. G.; Barich, D. H.; Nicholas, J. B. *J. Am. Chem. Soc.* **2000**, *122*, 12561.